# Anion Chelation-Induced Porphyrin Protonation and Its Application for Chloride Anion Sensing

**Ying Zhang, Mei Xian Li, Meng Yuan Lü, Rong Hua Yang,* Feng Liu, and Ke An Li**

*College of Chemistry and Molecular Engineering, Peking University, Beijing, 100871, China*

*Received: January 30, 2005; In Final Form: May 14, 2005*

The protonation of a simple *meso*-tetraphenylporphyrin in an organic−aqueous system was found to be induced by the counteranions. During the process of protonation, the counteranion of the proton sources binds with the porphyrin core and thus promotes the complexation of the porphyrin and protons. The interaction of porphyrin and anion was characterized by fluorescence, UV−visible, cyclic voltammetry, $^1$H NMR, and IR. Moreover, it could be exploited in selective fluorescent sensing of $Cl^-$. The sensing mechanism was based on extraction of protons from the aqueous phase into the organic phase by free base porphyrin and simultaneous coextraction of $Cl^-$, which promoted porphyrin protonation, and hence resulted in significant changes of the porphyrin fluorescence spectra. Selectivity trends turned out to be dependent upon the lipophilicity of anion and the binding affinity and structure complementarity between the protonated porphyrin and anions. The fluorescence enhancement of the porphyrin band at 684 nm showed modest selectivity for $Cl^-$ and $NO_3^-$.

Porphyrins are very important natural and synthetic compounds. Naturally occurring porphyrins play a vital role in the maintenance of both animal and plant bodies, because they constitute the basis of the respiratory system. Since porphyrins play an important part in many processes, such as photoinduced electrons transfer reaction (PET)[1] and photodynamic therapy (PDT),[2] studies of the properties and applications of porphyrin analogues have been particularly interesting in the fields of chemistry and biochemistry for a long time. On one hand, much work has been focused on metalloporphyrins complexes[3−10] that are widely used as catalysts,[7] carriers for anion-selective electrodes,[8] and receptors for the neutral molecules.[9] On the other hand, increasing attention has been paid to a class of porphyrin analogues with contracted and expanded porphyrins. In recent years, considerable efforts have been devoted to developing free base porphyrin derivatives as anion receptors and sensors. Sessler and co-workers have done excellent work in this field.[2,11−15] For example, sapphyrin, a member of a class of pentapyrrolic macrocycles, initially discovered by Woodward and his group,[16] has been shown to be highly selective receptors for anions[11c,d,13−15,17] and carriers for transporting different ionic and neutral species.[18] Furthermore, due to its unique photochemical and electrochemical properties,[19] in a series of artificial host molecules, porphyrin units were widely used as molecular platforms.[1a,20]

Free base porphyrins, such as *meso*-tetraphenylporphyrin ($H_2$TPP), representing conjugated tetrapyrrolic macrocycles, are well-characterized by the arrangement of four inward-pointing nitrogens in the core. The two imine nitrogens of a free base porphyrin are able to accept two protons to produce diprotonated species ($H_4TPP^{2+}$).[21] Due to the significance of protons in many essential biological processes and the effect of protonation on the porphyrin chemical and biological functions, in the past decades, a number of workers have studied porphyrin protonation interaction either in aqueous solution or in organic−aqueous systems,[3a,22−24] using spectrophotometric or potentiomertic techniques.[21,23,25−27] The acids employed for the protonation included glacial acetic acid,[27] pyridinesulfuric acid,[25,26] hydrochloric acid,[23,26] trifluoroacetic acid,[23,24b] and perchloric acid.[23] The differences in physical and chemical properties of the protonated species were observed by using different acids. For example, Aronoff and co-worker[26] have early noted that, in an inert solvent, free base porphyrin exhibited different UV−visible spectra in the presence of sulfuric acid and hydrochloric acid in aqueous solution. Segawa et al.[28] have also recently observed that the *J*-aggregations of a protonated water-insolube porphyrin in $CH_2Cl_2$ were formed in the presence of sulfuric acid, whereas the aggregations could not be formed in the solvent when hydrochloric acid or nitric acid was employed. However, no one so far has sensed the role of counteranions in porphyrin protonation, saying nothing of making any intensive investigation on the interactions between protonated porphyrins and counteranions systematically. Considering these facts, we are interested in the questions of (i) whether the porphyrin protonation could be affected by the counteranions; (ii) if so, how do the anions interact with the protonated porphyrin species; and (iii) to the extent it was observed, how this interaction may be exploited as an anion fluorescent sensor.

The present work was performed with the aim of investigating the questions proposed above. First, we studied the porphyrin protonation systematically in the presence of different anions in an organic−aqueous system and found that different anions caused distinctive spectroscopic and electroscopic features. This undoubtedly demonstrates that the protonated form of the $H_2$-TPP system does interact with anions that induce the porphyrin protonation. Initial evidence that the protonated porphyrin was capable of anion binding was derived from fluorescence, UV−visible, cyclic voltammetry, $^1$H NMR, and IR methods. Furthermore, we found that the fluorescence emission enhancement of the protonated porphyrin at 684 nm showed modest specificity

* To whom correspondence should be addressed. Fax: +86-10-62751708. E-mail: Yangrh@pku.edu.cn.

10.1021/jp050516a CCC: $30.25 
Published on Web 08/02/2005

to $Cl^-$ and $NO_3^-$. This finding led to the suggestion that this system may function as an anion fluorescent sensor.

## Experimental Section

**Materials and Reagents.** *meso*-Tetraphenylporphyrin ($H_2$-TPP) was synthesized according to the literature method.[29] The stock solution of $H_2TPP$ was prepared in $CH_2Cl_2$, and the concentration of $H_2TPP$ was less than $1.01 \times 10^{-5}$ M in order to avoid aggregation.[11c] The potassium salts of all anions studied were of analytical reagent grade and used without further purification. All salt solutions were prepared with doubly distilled water.

For IR, $^1H$ NMR, and cyclic voltammetry (CV) experiments, the porphyrin species without or with chloride ion (or other anions) was prepared as following: $H_2TPP$ (18.4 mg, 0.030 mmol) was dissolved in 3.0 mL of $CH_2Cl_2$, 2.0 mL of 0.5 M $H_2SO_4$ without or with 1.0 M KCl (or other salts of different anions) was added into the $CH_2Cl_2$ solution, and the overall solution was shaken vigorously for a few minutes. After 3 h, the organic layer was separated off and dried over sodium sulfate. Then, it was thoroughly dried in vacuo at 80 °C for further use.

**General Methods.** Fluorescence emission spectra were performed on a Hitachi F-4500 fluorescence spectrofluorometer (Kyoto, Japan) with the excitation and emission slits of 5.0 nm. UV−visible spectra were taken on a Hitachi U-3010 UV−vis spectrophotometer (Kyoto, Japan). The absorption and fluorescence measurements were carried out in a $CH_2Cl_2-H_2O$ system in which $H_2TPP$ was dissolved in 2.0 mL of $CH_2Cl_2$, a certain concentration of sulfuric acid with or without inorganic salts was added into the 0.5-mL aqueous phase, and then the absorption or fluorescence spectroscopy of porphyrin in $CH_2Cl_2$ was measured. The measurement parameters of the UV−vis spectrophotometer were set as follows: sampling interval, 1.00 nm; slit width, 1 nm; and scan speed, 600 nm/min. IR spectra were conducted on the Nicolet Magna-IR 550 spectrometer. $^1H$ NMR spectra were recorded on an Invoa-400 spectrometer at 298 K. All samples for $^1H$ NMR analysis were prepared in 5 mm NMR tubes using $CDCl_3$ as solvent with tetramethylsilane (TMS) as internal standard.

CV was performed with a BAS-100B electrochemical analyzer with a conventional three-electrode cell. The working electrode was a Pt electrode with a diameter of 1 mm. An Ag/AgCl wire and a platinum electrode were used as the reference and the auxiliary electrode, respectively. All potentials in this work were referenced to the redox potential of ferrocene. The solvent used was $CH_2Cl_2$. $Bu_4NPF_6$ (electrochemical grade) was obtained from Fluka. All electrochemical experiments were conducted under nitrogen atmosphere at the ambient temperature (298 K).

## Results and Discussion

**Protonation of Porphyrin in an Organic−Aqueous System.** Free base porphyrin with two proton-ionizable pyrrole nitrogen atoms behaves as a polyprotic acid. When an organic solution containing a free base porphyrin and an aqueous acid solution are put into contact, the protonation takes place at the liquid−liquid interface.[28,30] The stepwise acid−base equilibria for the porphyrin can be written as

$$H_4L^{2+} \overset{K_{a1}}{\rightleftharpoons} H_3L^+ + H^+ \quad (1)$$

$$H_3L^+ \overset{K_{a2}}{\rightleftharpoons} H_2L + H^+ \quad (2)$$

$$H_2L \overset{K_{a3}}{\rightleftharpoons} HL^- + H^+ \quad (3)$$

$$HL^- \overset{K_{a4}}{\rightleftharpoons} L^{2-} + H^+ \quad (4)$$

The neutral form of porphyrin ($H_2L$) can be successively protonated to form monocationic ($H_3L^+$) and dicationic ($H_4L^{2+}$) forms or successively deprotonated to produce monoanionic ($HL^-$) and dianionic ($L^{2-}$) forms. The deprotation of $H_4L^{2+}$ to $L^{2-}$ can pass through a host of alternate intermediates, the distribution of which is dependent on several factors, including the cation, ionic strength, and polarity of the environment. Since our experiments were carried out in acid solution, it was mainly concerned with the equilibria of eqs 1 and 2.

In comparison with other proton transfers from nitrogen acids, proton transfer from the diprotonated form of $H_2TPP$ is exceptionally slow. This may arise because the reaction is strongly disfavored thermodynamically.[21b] Thus, the monoprotonated form of porphyrin is difficult to detect under the present conditions.

**Effects of Anions on Porphyrin Protonation.** To investigate the effects of anions on porphyrin protonation in an organic−aqueous system, sulfuric acid was chosen as the proton source in the aqueous phase, since the sulfate anion tightly binds with water molecules and the amount of extraction into organic phase could be negligible.[28] In less polar solvent, such as $CH_2Cl_2$, $H_2TPP$ showed a fluorescence emission maximum at 651 nm,[31] and the fluorescence change at this wavelength in the presence of 0.5−1.5 M $H_2SO_4$ was virtually unobservable (Figure 1a−d), indicating that little protonated porphyrin species existed. In contrast, upon addition of the same concentration of $H_2SO_4$ containing 0.1 M of KCl to the $H_2TPP$ solution, significant fluorescence decreases were observed (Figure 1b′−d′). On the other hand, without sulfuric acid, no decrease of $H_2TPP$ fluorescence at 651 nm was observed upon the addition of KCl solution, even at high concentration, which demonstrated that $Cl^-$ would not interact with $H_2TPP$ in the absence of proton. In addition, it was also found that the fluorescence emission of the protonated porphyrin exhibited quite different behaviors in the presence of different anions (vide infra). These results led us to conclude that the counteranions had profound effects on porphyrin protonation.

The effect of anions on porphyrin protonation was further confirmed by UV−visible spectra. Figure 2 shows the absorption spectra of $H_2TPP$ at different conditions. Curve a was measured without any acid in the aqueous phase, and the maximum of the Soret band of $H_2TPP$ in $CH_2Cl_2$ occurred at 417 nm. Upon addition of 3.0 M $H_2SO_4$ to the aqueous phase, the absorbance at the 417 nm peak decreased with a red shift of the Soret band to 438 nm (Soret band of the protonated monomer) (curve b). When different anions were added to the $H_2SO_4$ solution, $H_2$-TPP showed different absorption response behaviors. In the presence of $F^-$, the absorption spectrum either at 417 nm or at 438 nm was less changed with respect to that in the presence of sulfuric acid, indicating that the interaction between $F^-$ and the protonated porphyrin was very weak. By contrast, when $NO_3^-$ or $Cl^-$ was added to the acidic solution, strong decreases of absorbance around 416 nm accompanied with the intense bands centered at 438 nm (curve d) or 446 nm (curve e), respectively, appeared. $NCS^-$ showed the similar effect on the

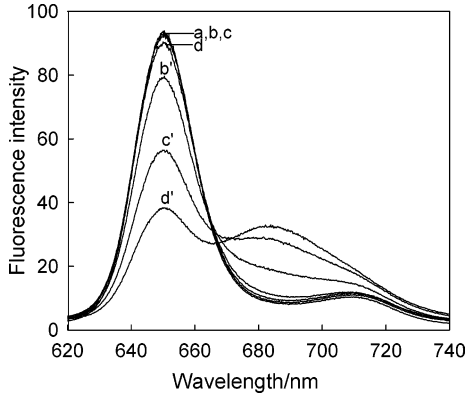


**Figure 1.** Effects of different concentrations of $H_2SO_4$ on $H_2TPP$ ($1.01 \times 10^{-5}$ M) fluorescence emission spectra ($\lambda_{ex} = 430$ nm) in $CH_2Cl_2$ in the absence (a−d) and presence (b′−d′) of 0.1 M KCl. $H_2SO_4$ concentration: a, 0; b and b′, 0.5 M; c and c′, 1.0 M; d and d′, 1.5 M.

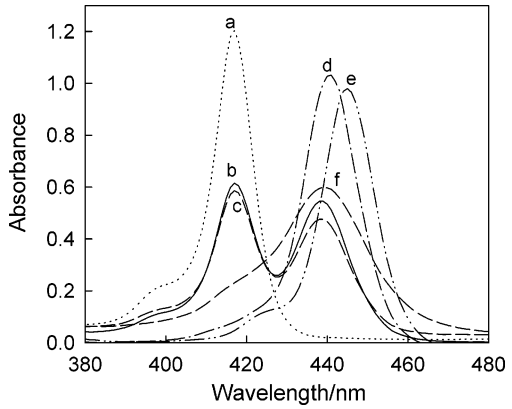


**Figure 2.** Effects of different anions on the UV−visible absorption spectra of the diprotonated form of porphyrin recorded in $CH_2Cl_2$: (a) $H_2TPP$ in 1.0 mL of $CH_2Cl_2$; (b) spectrum a conditions + 0.1 mL of 3.0 M $H_2SO_4$; (c) spectrum b conditions + KF; (d) spectrum b conditions + $KNO_3$; (e) spectrum b conditions + KCl; (f), spectrum b conditions + KNCS. $[H_2TPP] = 1.2 \times 10^{-6}$ M; [anions] = 9.0 mM.

**TABLE 1: Maximum Absorption Positions, Molar Absorption Coefficients, and Association Constants of the Protonated Porphyrins with Anions**

| anion | $\lambda_{max}$ (nm) | $\epsilon$ ($cm^{-1}$ $M^{-1}$) | $K$ ($M^{-2}$) |
|---|---|---|---|
| $SO_4^{2-}$ | 439 | $5.8 \times 10^4$ | $(1.5 \pm 0.2) \times 10^4$ [a] |
| $F^-$ | 438 | $9.6 \times 10^4$ | —[b] |
| $Cl^-$ | 446 | $5.58 \times 10^5$ | $(1.5 \pm 0.2) \times 10^5$ [c] |
| $Br^-$ | 449 | $5.14 \times 10^5$ | $(1.1 \pm 0.2) \times 10^5$ [a] |
| $H_2PO_4^-$ | 440 | $4.20 \times 10^5$ | $(8.7 \pm 0.3) \times 10^4$ [c] |
| $NO_3^-$ | 440 | $4.47 \times 10^5$ | $(1.1 \pm 0.1) \times 10^7$ [c] |
| $NCS^-$ | 439 | $2.09 \times 10^5$ | $(8.2 \pm 0.2) \times 10^7$ [a] |
| $ClO_4^-$ | 439 | $2.90 \times 10^5$ | —[b] |

[a] The association constants were acquired according to $H_2TPP$ fluorescence decreases at 684 nm. [b] The association constants could not be acquired under this condition. [c] The association constants were acquired according to $H_2TPP$ fluorescence enhancements at 684 nm.

porphyrin absorption spectroscopy as that of $NO_3^-$ or $Cl^-$; however, the absorbance enhancement at 438 nm was smaller than that of $NO_3^-$ or $Cl^-$. Additional spectral properties of $H_4TPP^{2+}$ in the presence of different anions are summarized in Table 1, which further demonstrate that the counteranions have complicated interactions with $H_2TPP$ during protonation.

Figure 3 shows the absorption spectra changes of $H_2TPP$ in the presence of different amounts of KCl in 1.5 M $H_2SO_4$. The maximum Soret band of $H_2TPP$ without $H_2SO_4$ occurred at 416 nm (the dashed line). Upon the addition of 1.5 M $H_2SO_4$, a small decrease (4.3%) of the Soret band absorption was

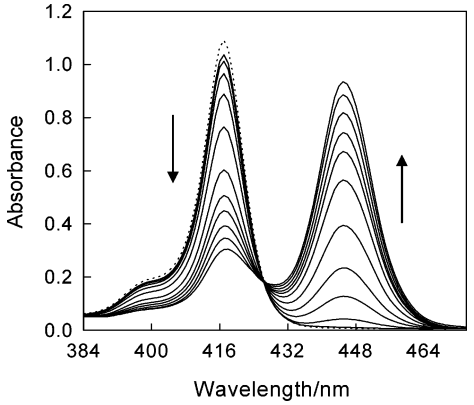


**Figure 3.** Absorption spectra of $H_2TPP$ in the presence of 1.5 M $H_2SO_4$ upon addition of increasing amounts of chloride ion. The dashed line corresponds to $1.2 \times 10^{-6}$ M $H_2TPP$ in 2.0 mL of $CH_2Cl_2$ without $H_2SO_4$. The arrows indicate the signal changes as increases in chloride ion concentrations (0, 0.119, 0.383, 0.763, 1.14, 1.51, 2.16, 2.90, 3.70, 4.41, 4.80 mM).

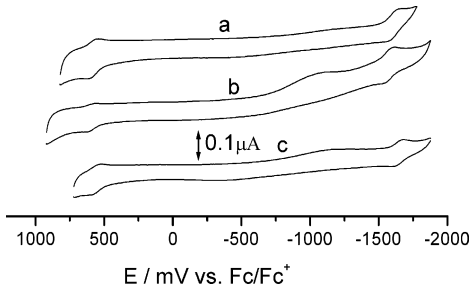


**Figure 4.** Cyclic voltammetry of $H_2TPP$ (curve a), $H_2TPP-H_2SO_4$ (curve c), $H_2TPP-H_2SO_4-Cl^-$ (curve b) in $CH_2Cl_2$ solution containing 0.1 M $n$-$Bu_4NPF_6$. Scan rate: 100 mV/s.

observed. However, addition of increasing aliquots of KCl to the acid solution caused not only a significant hypochromicity (72.1%, 4.8 mM KCl) of the 416-nm Soret band but also bathochromic shifts both of the 438-nm Soret band (∼8 nm) and the 648-nm Q-band (∼13 nm) (omitted) with a clear isobestic point at 426 nm. In addition, no absorbance changes at 475 and 725 nm (absorption bands of $H_4TPP^{2+}$ aggregations[28]) appeared, suggesting no porphyrin aggregates in the presence of $Cl^-$. These spectroscopic changes further indicate that the chloride anion acts as an important element interacting with the protonated porphyrin and makes a complex influence on the porphyrin protonation.

The electrochemical properties of protonated porphyrin are influenced by different anions. Figure 4 shows the CV of porphyrin in the presence of $SO_4^{2-}$ and $Cl^-$ in $CH_2Cl_2$ solution containing 0.1 M $n$-$Bu_4NPF_6$. Two couples of redox peaks, which correspond to one-electron-transfer reversible oxidation and reversible reduction of $H_2TPP$, respectively, according to literatures reported,[10,32] are observed in curve a. Curve c shows a new irreversible reduction peak with the addition of $H_2SO_4$, indicating the interaction between $H^+$ and $H_2TPP$, because no difference can be observed for $H_2TPP$ in the absence and presence of $HSO_4^-$. The CV for $H_4TPP^{2+}$-$Cl^-$ is also displayed in curve b, and one irreversible reduction peak is found, which is stronger compared with curve c. These results demonstrate that the chloride ion could further produce the protonation of porphyrin.

**Performance of Fluorescence Detection of $Cl^-$.** Figure 5 shows the influences of different concentrations of KCl on the fluorescence emission spectra of $1.01 \times 10^{-5}$ M $H_2TPP$ in $CH_2Cl_2$ solution containing sulfuric acid. The fluorescence change

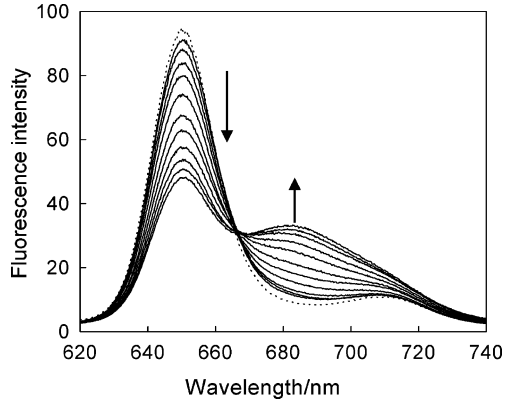


**Figure 5.** Fluorescence emission spectra of $H_2TPP$ in the presence of 1.5 M $H_2SO_4$ upon addition of increasing amounts of chloride ion. The dashed line corresponds to $1.01 \times 10^{-5}$ M $H_2TPP$ in 2.0 mL of $CH_2Cl_2$ without $H_2SO_4$. The arrows indicate the signal changes as increases in chloride ion concentrations (0, 0.383, 0.763, 1.14, 1.52, 1.91, 2.26, 2.64, 3.02, 3.70, 5.45 mM). The excitation wavelength was 430 nm.

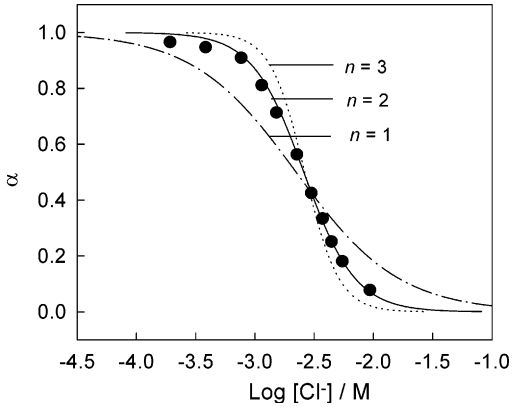


**Figure 6.** Response parameter values (α) as a function of the logarithm of $Cl^-$ concentrations. Theoretical response of $Cl^-$ was predicated by eq 6. The experimental data were fitted to the equation with the different complex ratios and equilibrium constants: (1) $n = 3$, $K = 5.5 \times 10^7$; (2) $n = 2$, $K = 1.5 \times 10^5$ (best fit); (3) $n = 1$, $K = 450$ (●, experimentally observed data points).

of $H_2TPP$ at 651 nm was small in the sulfuric acid solution. However, when aliquots of KCl were added, obvious decreases of the porphyrin emission at 651 nm and a red-shifted, structureless maximum centered at 683 nm were observed, which constitutes the basis for the fluorescence determination of $Cl^-$.

If the fluorescence response of $H_2TPP$ to $Cl^-$ results from the extraction of protons from aqueous phase into the organic phase by free base porphyrin and simultaneous co-extraction of $Cl^-$, the complex equilibrium of the porphyrin and $Cl^-$ at a two-phase system can be expressed as

$$n\mathrm{Cl}^-_{(aq)} + 2\mathrm{H}^+_{(aq)} + \mathrm{H_2TPP}_{(org)} \overset{K}{\rightleftharpoons} \mathrm{H_4TPPCl}_n^{\,2-n}{}_{(org)} \quad (5)$$

where the subscripts (aq) and (org) denote the aqueous and organic phase, respectively, and $K$ is the association constant. According to the derivation reported previously,[33] a response function for $Cl^-$ can be given as

$$[\mathrm{Cl}^-]^n = \frac{1}{K}\frac{1}{[\mathrm{H}^+]^2}\frac{1-\alpha}{\alpha} \quad (6)$$

where α is the ratio of the free concentration of porphyrin to the total concentration of the porphyrin in the system. α can be determined from the fluorescence changes at 683 nm[33]

$$\alpha = \frac{F - F_0}{F_1 - F_0} \quad (7)$$

where $F$ is the fluorescence intensity of the porphyrin actually measured at a defined $Cl^-$ concentration, $F_1$ is the fluorescence intensity of porphyrin in the sulfuric acid solution without $Cl^-$ ($\alpha = 1$), and $F_0$ is the fluorescence intensity when the porphyrin is completely complexed by $Cl^-$ ($\alpha = 0$). Detailed examination of the fluorescence intensity changes at 683 nm as a function of $[Cl^-]$ can determine the stoichiometry, $n$, and the association constant, $K$, using a curve-fitting method. Figure 6 shows the fitting of the titration data of Figure 5, which reveals a 1:2 porphyrin−chloride complex ($n = 2$), giving an association constant of $K = (1.5 \pm 0.2) \times 10^5$ $M^{-2}$. The fitting curve can serve as the calibration curve for the detection of chloride ion concentration. The association constants of porphyrin and other anions are summarized in Table 1.

Though the association constants that were determined according to the decreased or increased emission fluorescence

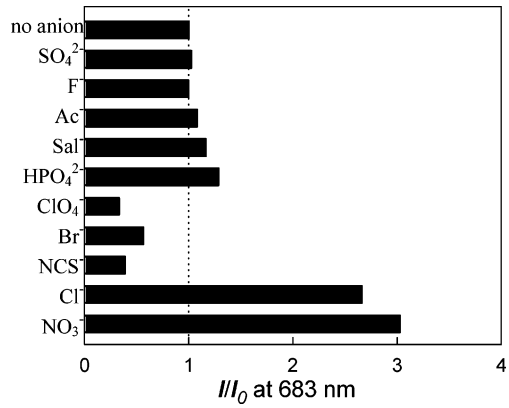


**Figure 7.** Fluorescence responses of $H_4TPP^{2+}$ against a 4.8 mM of various anions ($y$-axis markers) in the presence of 1.5 M $H_2SO_4$. $I_0$ and $I$ are emission intensities of the porphyrin at 683 nm in the $H_2SO_4$ solution in the absence and in the presence of anions, respectively. The excitation wavelength was 430 nm.

of $H_2TPP$ during the protonation process were adjacent (Table 1), the fluorescence enhancement of $H_2TPP$ at 683 nm is selective. Figure 7 summarizes the fluorescence signal change of $H_2TPP$ in $CH_2Cl_2$ in the presence of 1.5 M $H_2SO_4$ and 4.8 mM anions respectively, where $I_0$ and $I$ are the fluorescence intensities of the porphyrin in the absence and presence of anions. Reaction of $H_2TPP^{2+}$ with $Cl^-$ or $NO_3^-$ exhibits fluorescence intensity enhancement at 683 nm at the expense of the 651-nm band. Among other anions investigated, $F^-$, $Ac^-$, and $HPO_4^{2-}$ cause little effects on the $H_2TPP$ fluorescence emission at 683 nm with respect to that in the presence of $H_2SO_4$, whereas the fluorescence emissions of $H_2TPP$ at 683 nm are extensively quenched by $NCS^-$, $ClO_4^-$, or $Br^-$. The interactions of protonated porphyrin with anions may be dependent on the lipophilicity of anion and the binding affinity and structure complementarity between the protonated porphyrin and anions.[34] The fluorescence quenching of porphyrin by anions in the presence of $H_2SO_4$ may be attributed to further protonation of the porphyrin by anion binding interaction (vide infra) as well as the internal heavy-atom effect in which the anion promotes nonradiative deactivation of the excited singlet states via a spin−orbit coupling mechanism.[35]

The enhanced fluorescence of porphyrin by $Cl^-$ was not influenced by subsequent additions of a 200-fold excess of $SO_4^{2-}$, a 50-fold excess of $Ac^-$, a 20-fold excess of $F^-$, and a

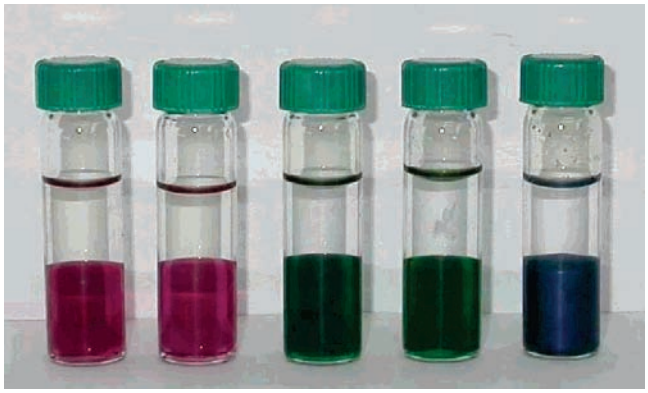

**Figure 8.** Color changes of $H_2TPP$ in $CH_2Cl_2$ induced by anions in the presence of 1.5 M $H_2SO_4$. The upper-layer from left to right are saturated KCl solution, 1.5 M $H_2SO_4$, and 1.5 M $H_2SO_4$ containing 1.0 M KCl, 1.0 M KBr, and 1.0 M $KNO_3$, respectively.

**TABLE 2: Analytical Results for Three Synthetic Samples**

| | sample composition ($\times 10^{-3}$ M) | determined ($\times 10^{-3}$ M)[a] | recovery (%) |
|---|---|---|---|
| 1 | KF, 15.2; NaAc, 15.2; $K_2SO_4$, 7.60; $Na_2HPO_4$, 3.04; $NaH_2PO_4$, 1.52; KCl, 1.52 | 1.51 | 99.3 |
| 2 | KF, 29.9; NaAc, 29.9; $K_2SO_4$, 15.0; $Na_2HPO_4$, 6.0; $NaH_2PO_4$, 3.0; KCl, 2.99 | 3.02 | 101 |
| 3 | KF, 81.9; NaAc, 81.9; $K_2SO_4$, 41.0; $Na_2HPO_4$, 8.2; $NaH_2PO_4$, 5.46; KCl, 5.46 | 5.84 | 107 |

[a] Average value of three determinations.

2-fold excess of $Br^-$. Although the fluorescence response of $H_4TPP^{2+}$ to $NO_3^-$ is also sensitive, distinguishing $NO_3^-$ and $Cl^-$ can be achieved via color changes by naked eye, which corresponds to blue and green color, respectively (Figure 8). Furthermore, for $Cl^-$ measurement in physiological environment, the amount of $NO_3^-$ is much lower than that of $Cl^-$. In reality, $NO_3^-$ would not significantly affect the measurement of $Cl^-$. The results are important and helpful in validation of the method to meet the selectivity requirements of a $Cl^-$ assay in physiological fields.

The fluorescence response of $H_2TPP$ to anion depends on the acidity of the aqueous phase. In neutral or alkaline medium, $H_2TPP$ could not bind with anions and thus could not cause any fluorescence response. $H_4TPP^{2+}$ responds to $Cl^-$ with modest sensitivity in the presence of 1.0−2.5 M $H_2SO_4$ in aqueous phase. Changing the acidity of the measuring solution below 1.0 M $H_2SO_4$ results in a shift of the dynamic range to higher chloride concentration. On the other hand, increasing the $H_2SO_4$ concentration over 2.5 M lowers the detection limit for $Cl^-$; however, the sensitivity (response slope) also reduces. The volume of the aqueous phase also affects the response. Fixing the volume of $CH_2Cl_2$ to be 2.0 mL, when the volume of the aqueous phase is more than 0.1 mL, we observed stable responses with high sensitivity. The recognition of chloride ion by $H_4TPP^{2+}$ should be carried out in an aqueous−organic phase system. In a mixed solution of ethanol and water, no regular fluorescence response was observed.

The preliminary application of the present method was tested by applying it for the determination of $Cl^-$ concentration in three synthetic samples in the presence of other interferents. The samples were prepared on the basis of possible existing anions in a physiological environment. The results are given in Table 2, and the recoveries of the three samples are 99.3−107%.

**Study on the Interaction Mechanism between Protonation Porphyrin and Anion.** As the starting point, there are interactions between protonated porphyrin and anions that promote the porphyrin protonation; however, the question of how the anion interacts with the protonated porphyrin has not been clarified. Besides the lipophilicity of the anions, it is expected that the determining factors for protonated porphyrin−anion interaction would be mainly governed by (i) the electrostatic action of ion pairing, (ii) a combination of electrostatic action and hydrogen-bonding interaction between the pyrrolic NH protons of porphyrin and an anion, and (iii) an almost purely hydrogen-bonding interaction. Evidences for different kinds of interacting modes can be obtained from $^1H$ NMR and IR spectra.

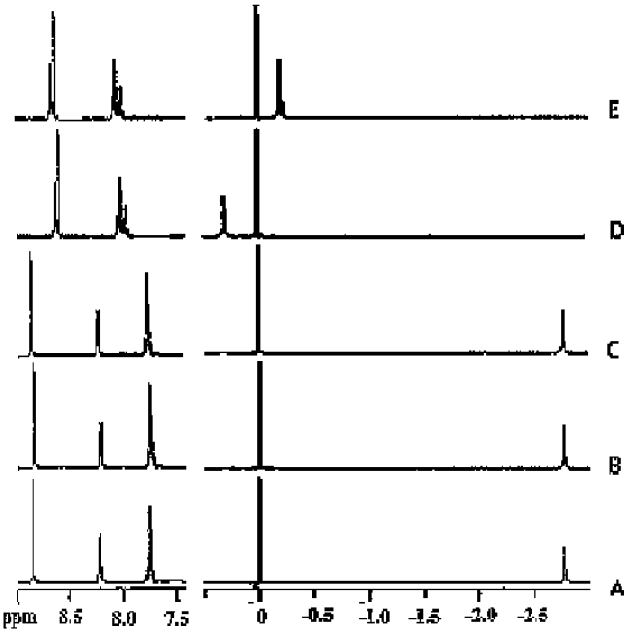


**Figure 9.** Portions of $^1$ H NMR of $H_2TPP$ in the absence (A) and presence (B) of $H_2SO_4$ and in $H_2SO_4$ containing different salts: KF (C), KCl (D) and KBr (E). The signals observed between 0 to −2.8 and 7.5 to 9.0 ppm are assigned to pyrrolic N*H* protons and aromatic protons, respectively.

Figure 9 shows the $^1H$ NMR spectra of protonated porphyrin species with different counteranions. In $CDCl_3$, $H_2TPP$ yielded a chemical shift for the pyrrolic N*H* protons of −2.76 ppm (spectrum A). However, in the case of KCl and KBr, the pyrrolic N*H* protons were shifted to 0.297 and −0.209 ppm (spectra D and E), respectively. It is indicative of the essential role of anion recognition process via hydrogen bonding.[34] In addition, it was observed that the $\beta$-pyrrolic C*H* proton signals shifted upfield ($\Delta\delta$ = 0.18 ppm), whereas the signals of the protons of *meso*-phenyl moieties shifted downfield ($\Delta\delta$ = 0.23−0.42 ppm) in the presence of KCl and KBr. Since anion binding to the pyrrolic N−H groups is expected to increase the electronic density on the pyrrole ring and engender upfield shifts in the $\beta$-pyrrolic C*H* proton signals,[36] the relatively large upfield shift of the $\beta$-pyrrolic C*H* protons may come from the increased charge neutralization provided by central anions binding rather than simple "external" ion paring electrostatic attraction.[11a,c,34]

The key predicative ideal of IR is the N−H stretching frequency (Figure 10). The N−H stretching frequency, which usually occurs at 3500 $cm^{-1}$ for the pyrrole module, occurs at 3306 $cm^{-1}$ for the porphine nucleus, indicating that, in the free base of the porphyrin, the two protons are held in intramolecular hydrogen bonds.[37] In contrast, in the presence of $Cl^-$, the N−H stretching frequency returned to 3523 $cm^{-1}$, which indicates that the intramolecular N···H hydrogen bonds of the former porphine nucleus were somewhat decreased due to reaction of $Cl^-$ with the NH protons. The increase in the stretching frequency is ascribed to three facts: (i) the intramolecular NH

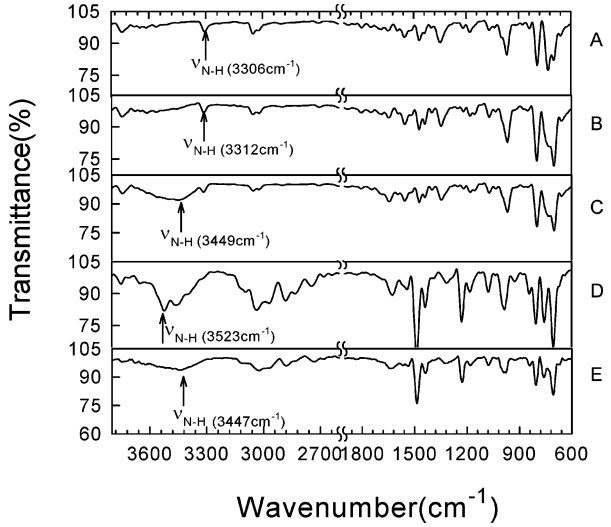


**Figure 10.** Portions of IR spectra of $H_2TPP$ in the absence (A) and presence (B) of $H_2SO_4$ and in $H_2SO_4$ containing different salts: KF (C), KCl (D) and KBr (E)

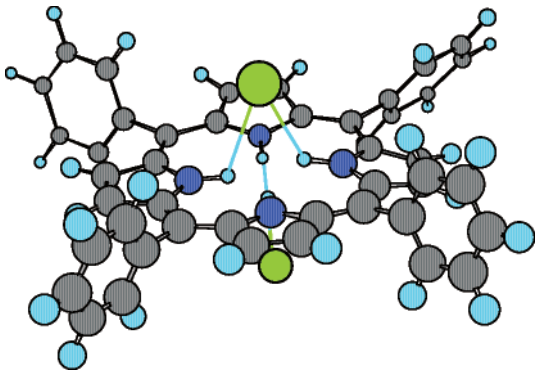

**Figure 11.** Schematic graph of protonated porphyrin species interacted with chloride anion. The green atoms represent chloride anion.

hydrogen bonds of the former porphine nucleus are somewhat decreased by the formation of NH···Cl hydrogen bonds; (ii) interacting with $Cl^-$, the central protons are tied up tightly in nitrogen-to-chloride anion hydrogen bonds, thereby reducing the ability of the NH groups to act as vibrational energy sinks;[38] and (iii) The formation of the NH···Cl hydrogen bonds destroyed the conjugation of the porphine plane.

On the basis of the relative size of the porphine nucleus and chloride ion (atomic radii 1.67 Å[39]) and the nonplanar conformation of the $H_4TPP^{2+}$ skeleton,[23,40] we thus propose a molecular modeling structure using Chemoffice 7.0 MM2 utilities (Figure 11). It reveals that the presence of two chloride anions are combined in a nearly symmetric fashion above and below the face of the porphine core, held in place by two hydrogen bonds.[11a]

## Conclusion

It might be mentioned at this point that there is an abundance of literature on porphyrin complexes and protonated porphyrins; however, conspicuous gaps are still seen with respect to the properties of the protonated porphyrin. The present results serve to highlight the facts that the protonated porphyrin does have special interactions with definite anions, which, in turn, promote porphyrin protonation. The influence of anions on porphyrin protonation in aqueous−organic phase may be determined by the lipophilicity of the counteranions and the hydrogen-bonding interaction between the protonated species and the anions. The selective interactions of $Cl^-$ and the protonated porphyrin may be exploited as a $Cl^-$ fluorescent sensor. The immobilization of the porphyrin to the fiber optic surface, which may lead to a practically useful $Cl^-$ sensing device, is currently underway in our laboratory, and the results will be reported.

**Acknowledgment.** Financial support from the National Science Foundation of China (Grant No. 20475005) is gratefully acknowledged.

## References and Notes

(1) (a) Wasielewski, M. R. *Chem. Rev.* **1992**, *92*, 435−461. (b) Kuroda, Y.; Ito, M.; Sera, T.; Ogoshi, H. *J. Am. Chem. Soc.* **1993**, *115*, 7003−7004. (c) Fukuzumi, S.; Ohkubo, K.; E, W. B.; Shao, J. G.; Kadish, K. M.; Hutchison, J. A.; Ghiggino, K. P.; Sintic, P. J.; Crossley, M. J. *J. Am. Chem. Soc*. **2003**, *125*, 14984−14985.

(2) Bonnet, R. *Chem. Soc. Rev.* **1995**, *24*, 19−33.

(3) (a) Corwin, A. H.; Chivvis, A. B.; Poor, R. W.; Whitten, D. G.; Baker, E. W. *J. Am. Chem. Soc*. **1968**, *90*, 6577−6583. (b) Nagatani, H.; Iglesias, R. A.; Fermín, D. J.; Brevet, P.-F.; Girault, H. H. *J. Phys. Chem. B* **2000**, *104*, 6869−6876.

(4) deRege, P. J. F.; Williams, S. A.; Therien, M. J. *Science* **1995**, *269*, 1409−1413.

(5) For an overview, see: Arnold, D. P.; Blok, J. *Coord. Chem. Rev.* **2004**, *248*, 299−319.

(6) Lahiri, J.; Fate, F. D.; Ungashe, S. B.; Groves, J. T. *J. Am. Chem. Soc.* **1996**, *118*, 2347−2358.

(7) (a) Moghadam, M.; Tangestaninejad, S.; Mirkhani, V.; Shaibani, R. *Tetrahedron* **2004**, *60*, 6105−6111. (b) Suda, K.; Sashima, M.; Izutsu, M.; Hino, F. *J. Chem. Soc. Chem. Commun*. **1994**, 949−950. (c) Cheng, S.-H.; Su, Y. O. *Inorg. Chem*. **1994**, *33*, 5847−5854.

(8) (a) Amini, M. K.; Shahrokhian, S.; Tangestaninejad, S. *Anal. Chem.* **1999**, 71, 2502−2505. (b) Sharokhian, S.; Hamzehloei, A.; Bagherzadeh, M. *Anal. Chem*. **2002**, *74*, 3312−3320. (c) Hattori, H.; Hoshino, M.; Wakii, T.; Yuchi, A. *Anal. Chem*. **2004**, *76*, 5056−5062.

(9) (a) Antonisse, M. M. G.; Snellink-Ruël, B. H. M.; Engbersen, J. F. J.; Reinhoudt, D. N. *J. Chem. Soc.; Perkin Trans 2* **1998**, 773−777. (b) Zhang, Y.; Yang, R. H.; Liu, F.; Li, K. A. *Anal. Chem*. **2004**, *76*, 7336−7345.

(10) Tsuda, A.; Sakamoto, S.; Yamaguchi, K.; Aida, T. *J. Am. Chem. Soc.* **2003**, *125*, 15722−15723.

(11) (a) For an overview, see: Sessler, J. L.; Camiolo, S.; Gale, P. A. *Coord. Chem. Rev.* **2003**, *240*, 17−55. (b) Furuta, H.; Maeda, H.; Osuka, A. *Chem. Commun*. **2002**, 17, 1795−1804. (c) Shionoya, M.; Furuta, H.; Lynch, V.; Harriman A.; Sessler, J. L. *J. Am. Chem. Soc.* **1992**, *114*, 5714−5722. (d) Sessler, J. L.; Davis, J. M. *Acc. Chem. Res.* **2001**, *34*, 989−997.

(12) Caravan, P.; Ellison, J. J.; McMurry, T. J.; Lauffer, R. B. *Chem. Rev.* **1999**, *99*, 2293−2352.

(13) (a) Iverson, B. L.; Shreder, K.; Král, V.; Sansom, P.; Lynch, V.; Sessler, J. L. *J. Am. Chem. Soc*. **1996**, *118*, 1608−1606. (b) Král, V.; Andrievsky, A.; Sessler, J. L. *J. Am. Chem. Soc*. **1995**, *117*, 2953−2954.

(14) For examples of expanded porphyrins that act as selective anion receptors, see:(a) Král, V.; Sessler, J. L.; Furuta, H. *J. Am. Chem. Soc*. **1992**, *114*, 8704−8705. (b) Gale, P. A., Sessler, J. L., Král, V. *Chem. Commun*. **1998**, 1−8. (c) Gale, P. A., Sessler, J. L. *J. Am. Chem. Soc*. **1999**, *121*, 11020−11021. (d) Miyaji, H., Sato, W., Sessler, J. L. *Angew. Chem., Int. Ed.* **2000**, *39*, 1777−1780. (e) Sessler, J. L., Bleasdale, E. R., Gale, P. A. *Chem. Commun*. **1999**, 1723−1724.

(15) (a) Sessler, J. L.; Cyr, M. J.; Lynch, V. *J. Am. Chem. Soc*. **1990**, *112*, 2810−2813. (b) Sessler, J. L.; Andrievsky, A.; Král, V.; Lynch, V. *J. Am. Chem. Soc*. **1997**, *119*, 9385−9392.

(16) Bauer, V. J.; Clive, D. L. J.; Dolphin, D.; Paine, J. B.; Harris, F. L., III; King, M. M.; Loder, J.; Wang, S. W. C.; Woodward, R. B.; *J. Am. Chem. Soc*. **1983**, *105*, 6429−6436.

(17) (a) Turner, B., Botoshansky, M., Eichen, Y. *Angew. Chem., Int. Ed*. **1998**, *37*, 2475−2478. (b) Cafeo, G., Kohnke, F. H., LaTorre, G. L., White, A. J. P., Williams, D. J. *Angew. Chem., Int. Ed*. **2000**, *39*, 1496−1498.

(18) For an overview, see: Ravikumar, M.; Chandrashekar, T. K. *J. Inclusion Phenom. Macrocyclic Chem.* **1999**, *35*, 553−582.

(19) (a) Kuroda, Y.; Kado, Y.; Higashioji, T.; Hasegawa, J.; Kawannami, S.; Takahshi, M.; Shiraishi, N.; Tanabe, K.; Ogoshi, H. *J. Am. Chem. Soc*. **1995**, *117*, 10950−10958. (b) Jagessar, R. C.; Shang, M.; Scheidt, W. R.; Burns, D. H. *J. Am. Chem. Soc*. **1998**, *120*, 11684−11692. (c) Ogoshi, H.; Mizutani, T. *Acc. Chem. Res*. **1998**, *31*, 81−89.

(20) (a) Hayashi, T.; Miyahara, T.; Koide, N.; Kato, Y.; Masuda, H.; Ogoshi, H. *J. Am. Chem. Soc.* **1997**, *119*, 7281−7290. (b) Aoyama, Y.; Asakawa, M.; Matsui, Y.; Ogoshi, H. *J. Am. Chem. Soc.* **1991**, *113*, 6233−6240.

(21) (a) Aronoff, S. *J. Phys. Chem*. **1958**, *62*, 428−431. (b) Hibbert, F.; Hunt, K. P. P. *J. Chem. Soc. Perkin 2* **1977**, 1624.

(22) (a) Finikova, O.; Galkin, A.; Rozhkov, V.; Cordero, M. *J. Am. Chem. Soc.* **2003**, *125*, 4882−4893. (b) Pasternack, R. F.; Huber, P. R.; Boyd, P.; Engasser, G.; Francesconi, L.; Gibbs, E.; Fasella, P.; Venturo, G. C.; Hinds, L. deC *J. Am. Chem. Soc.* **1972**, *94*, 4511−4517. (c) Baker, H.; Hambright, P. Wagner, L. *J. Am. Chem. Soc.* **1973**, *95*, 5942−5946.

(23) Stone, A.; Fleischer, E. B. *J. Am. Chem. Soc*. **1968**, *90*, 2735−2748.

(24) (a) Maity, D. K.; Bell, R. L.; Truong, T. N. *J. Am. Chem. Soc*. **2000**, *122*, 897−906. (b) Akins, D. L.; Zhu, H.-R.; Guo, C. *J. Phys. Chem*. **1996**, *100*, 5420−5425. (c) Udal' tsov, A. V.; Kazarin, L. A.; Sweshnikov, A. A. *J. Mole. Struc*. **2001**, *562*, 227−239.

(25) Aronoff, S.; Weast, S. A.; *J. Org. Chem*. **1941**, *6*, 550−557.

(26) Aronoff, S.; Calvin, M. *J. Org. Chem*. **1943**, *8*, 205−223.

(27) Conant, J. B.; Chow, B. F.; Dietz, E. M. *J. Am. Chem. Soc*. **1934**, *56*, 2185−2189.

(28) Okada, S.; Segawa, H. *J. Am. Chem. Soc*. **2003**, *125*, 2792−2796.

(29) Adler, A. D.; Longo, F. R.; Finarelli, J. D. *J. Org. Chem*. **1967**, *32*, 476.

(30) Nagatani, H.; Watarai, H. *Anal. Chem*. **1996**, *68*, 1250−1253.

(31) Under this condition, dimerization of $H_2$TPP is negligible (as confirmed by line Beer's law plots in the $1.0 \times 10^{-6}$ M to $5.0 \times 10^{-5}$ M regime).

(32) Kadish, K. M.; Xu, Q. Y.; Barbe, J.-M.; Anderson, J. E.; Wang E.; Guilard, R. *J. Am. Chem. Soc*. **1987**, *109*, 7705−7714.

(33) Yang, R. H.; Li, K. A.; Wang, K. M.; Zhao, F. L.; Li, N.; Liu, F. *Anal. Chem*. **2003**, *75*, 612−621.

(34) (a) Sancenón, F.; Martínez-Máñez, R.; Soto, J. *Angew. Chem., Int. Ed*. **2002**, *41*, 1416−1419. (b) Demeshko, S.; Dechert, S.; Meyer, F. *J. Am. Chem. Soc*. 2004, 126, 4508−4509.

(35) Fan, E.; van Arman, S. A.; Kincaid, S.; Hamilton, A. D. *J. Am. Chem. Soc*. **1993**, *115*, 369−370.

(36) Panda, P. K.; Lee, C.-H. *Org. Lett*. **2004**, *6*, 671−674.

(37) Thomas, D. W.; Martell, A. E. *J. Am. Chem. Soc*. **1956**, *78*, 1338−1343.

(38) Sessler, J. L.; Cyr, M.; Furuta, H.; Král, V. Mody, T.; Morishima, T.; Shionoya, M.; Weghorn, S. *Pure Appl. Chem.* **1993**, *65*, 393−398.

(39) Shannon, R. D. *Acta Crystallogr* **1976**, *A32*, 751−767.

(40) Fleischer, E. B. *Acc. Chem. Res*. **1970**, *3*, 105−112.